Towards development of a fiber optic-based transmission monitoring system

Chris S. Baldwin[♣a], Jason S. Kiddy[a], Paul D. Samuel[b]
[a]Aither Engineering, 4865 Walden Lane, Lanham, MD USA 20706
[b]Daedalus Flight Systems, 8945 N. Westland Dr., Suite 302
Gaithersburg, MD 20877

ABSTRACT

There is interest in the rotorcraft community to develop health monitoring technologies. Among these technologies is the ability to monitor the transmission planetary gear system. The gearbox environment does not lend itself to traditional sensing technologies due to the harsh environment and crowed space. Traditional vibration-based diagnostics are based on the output from externally mounted sensors, usually accelerometers fixed to the gearbox exterior. This type of system relies on the ability of the vibration signal to travel from the gears through the gearbox housing. These sensors are also susceptible to other interference including electrical magnetic interference (EMI). For these reasons, the development of a fiber optic-based transmission monitoring system represents an appealing alternative to the accelerometer due to their resistance to EMI and other signal corrupting influences. Aither Engineering has been working on integrating the fiber optic sensors into the gearbox environment to measure strain on the ring gear of the planetary gear system. This application utilizes a serial array of wavelength division multiplexed fiber Bragg grating (FBG) sensors. Work in this area has been conducted at both the University of Maryland, College Park and more recently at the NASA Glenn Research Center (NGRC) OH-58 transmission test rig facility. This paper discusses some of the testing results collected from the fiber optic ring gear sensor array. Based on these results, recommendations for system requirements are addressed in terms of the capabilities of the FBG instrumentation.

Keywords: Bragg Grating, Health Monitoring, Helicopter Transmission

1. INTRODUCTION

The health of internal stages of a planetary helicopter transmission has historically been difficult to diagnose due to the complex geometry of the planetary gearbox and the inability to directly monitor the rotating gears. An example of a planetary stage, as used in a helicopter transmission, is shown in Figure 1. The planetary stage consists of three main gear levels. The central gear is referred to as the sun gear and the three gears that rotate about the sun gear are called the planetary gears. The planetary gears are connected to a carrier plate, not shown, which provides the output to the system. In rotorcraft applications, the planetary gears ride within the stationary ring gear.

Typically for damage detection purposes, a small number of accelerometers are mounted externally to the gearbox housing to record the vibration signals. Gearbox fault detection algorithms make comparisons with nominal vibration test data to apply thresholds or seek pattern differences that may indicate problems in the transmission system. The hypothesis behind vibration-based techniques is that the gear defect will modulate the vibration under normal conditions, the modulated signal can be picked up by vibration sensors, and finally, the abnormal signal features can be extracted by further signal processing techniques. It has been shown that detection of planetary component faults can be aided by the use of various synchronous averaging algorithms [1,2], referred to as planetary vibration separation algorithms. However, these algorithms are based on the output from a single sensor and are susceptible to corruption from external disturbances [3]. These external disturbances can lead to false alarms or missed fault diagnoses.

Monitoring of dynamic systems with fiber optic sensors has been limited to date by the availability of sensing systems capable of providing adequate sampling rates and the desired sensor multiplexing capabilities. The most commonly used

♣ cbaldwin@aitherengineering.com; phone 1 240 296-1303; fax 1 240 296-1306; www.aitherengineering.com

dynamic systems have been based on interferometric techniques which provide high speed measurements but little opportunity for multiplexing. A key advantage of using fiber optic sensors for this project was the ability to multiplex many sensors onto the ring gear. Hence fiber Bragg Grating (FBG) sensors were chosen. During this research effort, a Micron Optics' sm130 interrogator was used to monitor a 13 FBG sensor array that was mounted to the outer surface of the ring gear at sampling rates of 1 kHz. In order to evaluate the benefits of higher sampling rates, a Smart Fibres' Smart Scan interrogator was used to collect comparison data for two operating conditions at a sampling rate of 20 kHz. The Smart Scan system was provided as a demonstration unit to Aither Engineering for this test. The research effort presented here is an extension of previous work conducted by Aither at the University of Maryland, College Park [4].

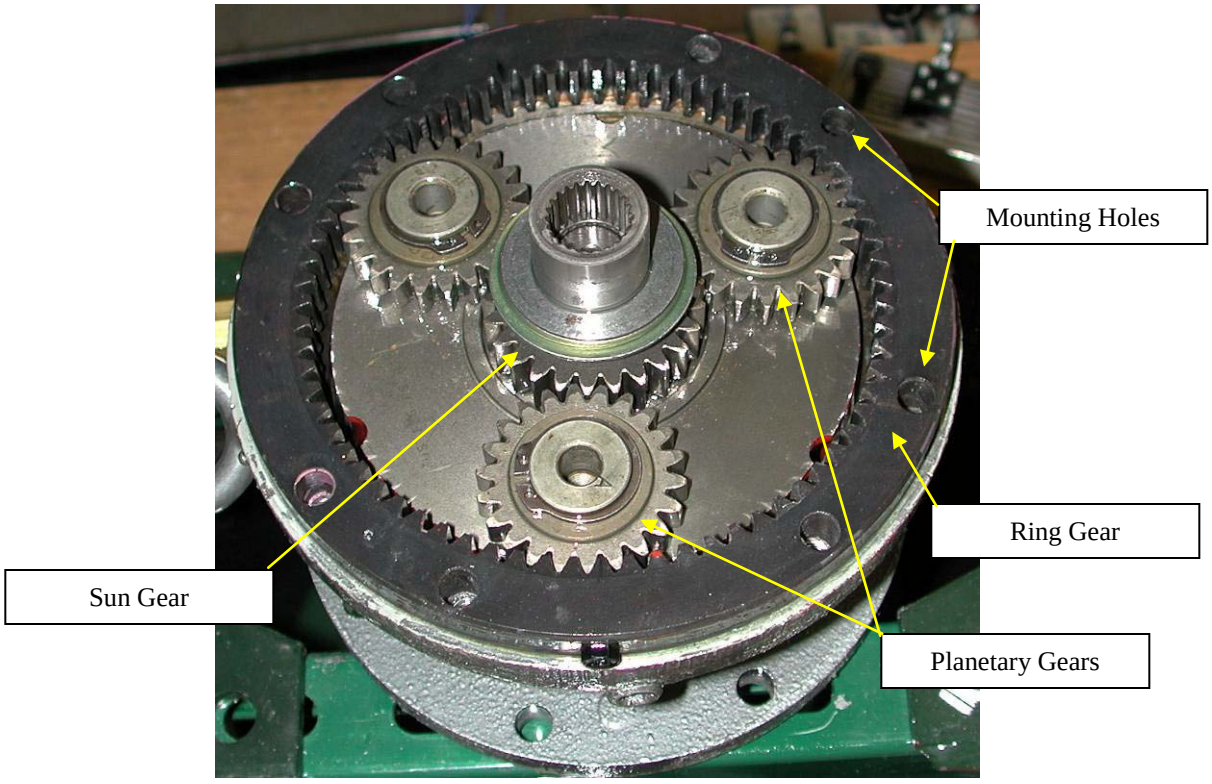

Figure 1: Example of a planetary gear assembly from University of Maryland test rig [4]

2. EXPERIMENTAL SETUP

The major goal of the program was to study data collected at the NASA Glenn Research Center (NGRC) OH-58 transmission test rig facility from the fiber optic ring gear sensor array and apply data processing techniques to evaluate damage detection algorithms. Multiple damage cases were tested under this program. After determination of the damage detection approach, the damage data was evaluated to ascertain how each type of damage is manifested in the signal, and how well each type of damage can be detected using the selected approach [5].

The transmission housing used for testing of the OH-58 transmission test rig is displayed in Figure 2. The ring gear is displayed with the optical fiber lead shown exiting the transmission housing at the oil port. The planetary gear assembly differs from the one tested previously at the University of Maryland in that the ring is not mounted to the transmission housing by bolts, but by spline teeth. Also, the OH-58 transmission system utilizes four planetary gears instead of three, as pictured in Figure 1. In order to incorporate the optical fiber leads and sensors into the transmission housing, a few

modifications were required including placing a groove in the oil input port for the optical fiber egress and machining a portion of the spline teeth from the ring gear for mounting the FBG sensor array.

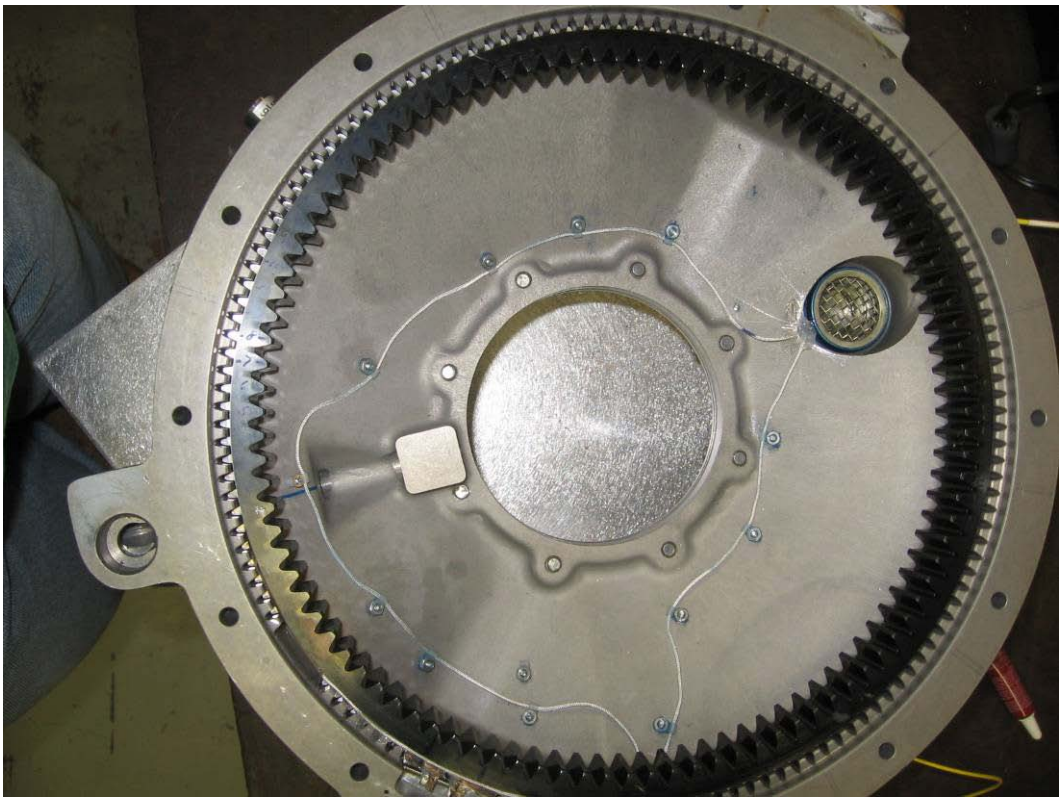

Figure 2: Transmission housing for the NASA Glenn Research Center OH-58 test rig with optical fiber path

The optical fiber leads that egressed from the transmission housing at the oil input port were connectorized to ease installation and hook up to the interrogation systems. Optical fiber patch cords were run from the OH-58 test rig to the adjacent control room where the interrogation systems were housed. For comparative data sampling, the transmission system was run at a steady state to minimize the influence of temperature variations due to the heating of the transmission components. Data was collected with one interrogator at a time with the optical fiber leads being manually switched from the sm130 to the Smart Scan system.

3. COMPARISON OF DATA SAMPLING RATES

For the comparison, only a small amount of data was collected in order to evaluate the quality and characteristics of the fiber optic strain vibration signals when sampled at a higher rate. Data was collected for two conditions 1 – normal operating RPM, high torque, no mast load and 2 – low RPM, high torque, no mast load using the Smart Scan interrogator with a sampling rate of 20 kHz. The most important advantage of the fiber optic high sampling rate data is the potential to perform damage detection at the normal operating RPM of the OH-58C transmission. Based on this and in the interest of space, only the normal operating condition will be presented in this paper.

Figure 3 presents a comparison of one carrier cycle of raw, unaveraged normal RPM data collected at 1 kHz and at 20 kHz. Figure 4 shows the high frequency components of the signals, and Figure 5 shows the low frequency components of the signals. The fiber optic strain signals contain both a high frequency component associated with tooth mesh deformations as well as a low frequency component associated with the deformation of the ring gear.

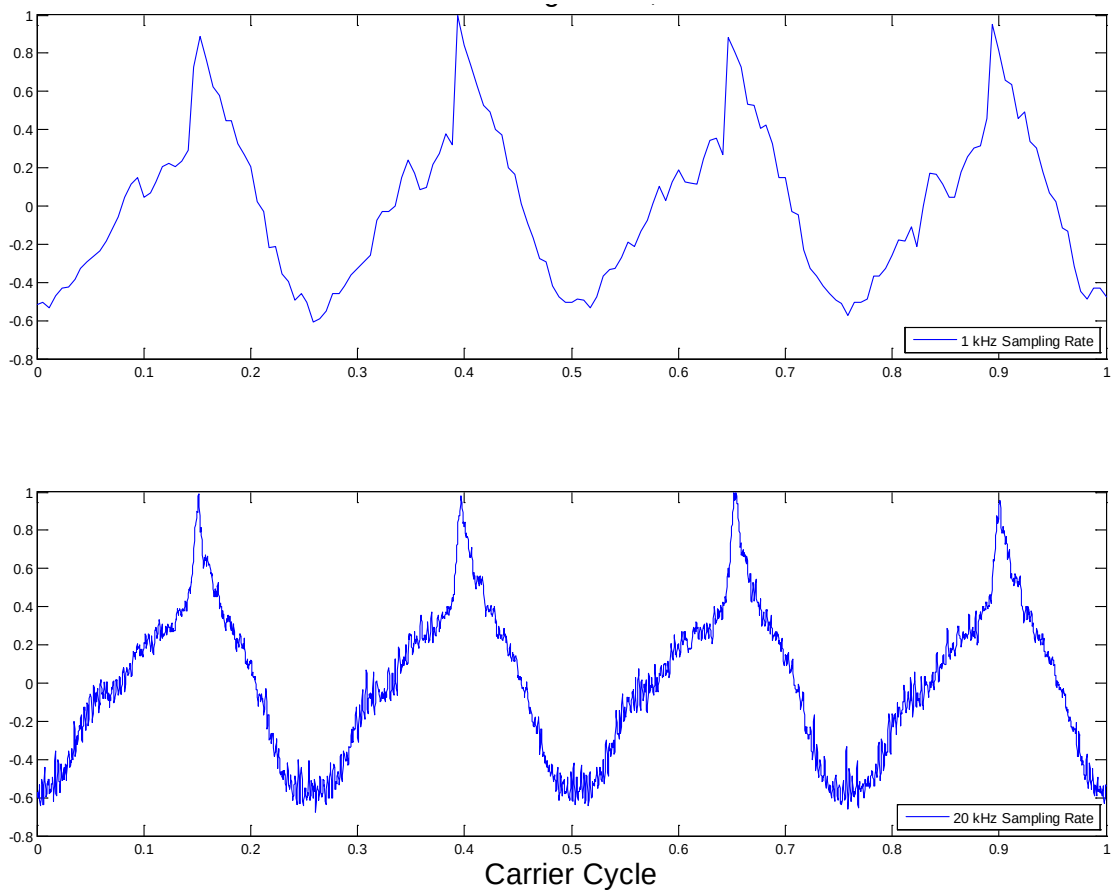

Figure 3: Raw data collected over 1 carrier rotation cycle: 1 kHz sampling rate (top) and 20 kHz sampling rate (bottom)

From these figures, it is evident that the high sampling rate data contains high frequency features that are not seen in the low sampling rate data and that the high sampling rate data more accurately and consistently captures the signal waveshape. It is clear that this improvement is at least in part due to a decrease in aliasing errors. The consistency of the waveshape is most evident in the low frequency signal. However, the lobes in the high sampling rate are even less prevalent in this case, indicating that averaging multiple cycles may be more advantageous when working with the high sampling rate data. Only a limited amount of high sampled rate data was able to be collected at a given time due to data buffering issues with the laptop used with the Smart Scan Interrogator.

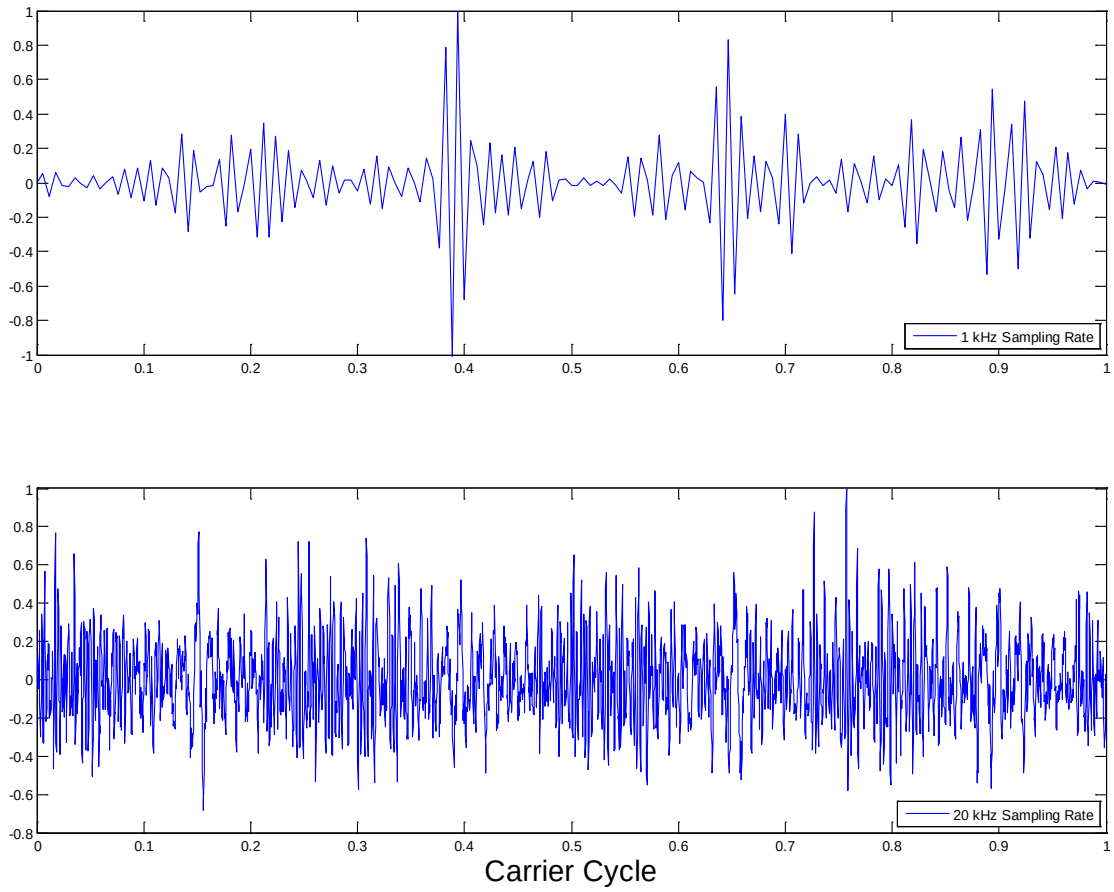

Figure 4: High frequency component of data collected over 1 carrier rotation cycle:1 kHz sampling rate (top) and 20 kHz sampling rate (bottom)

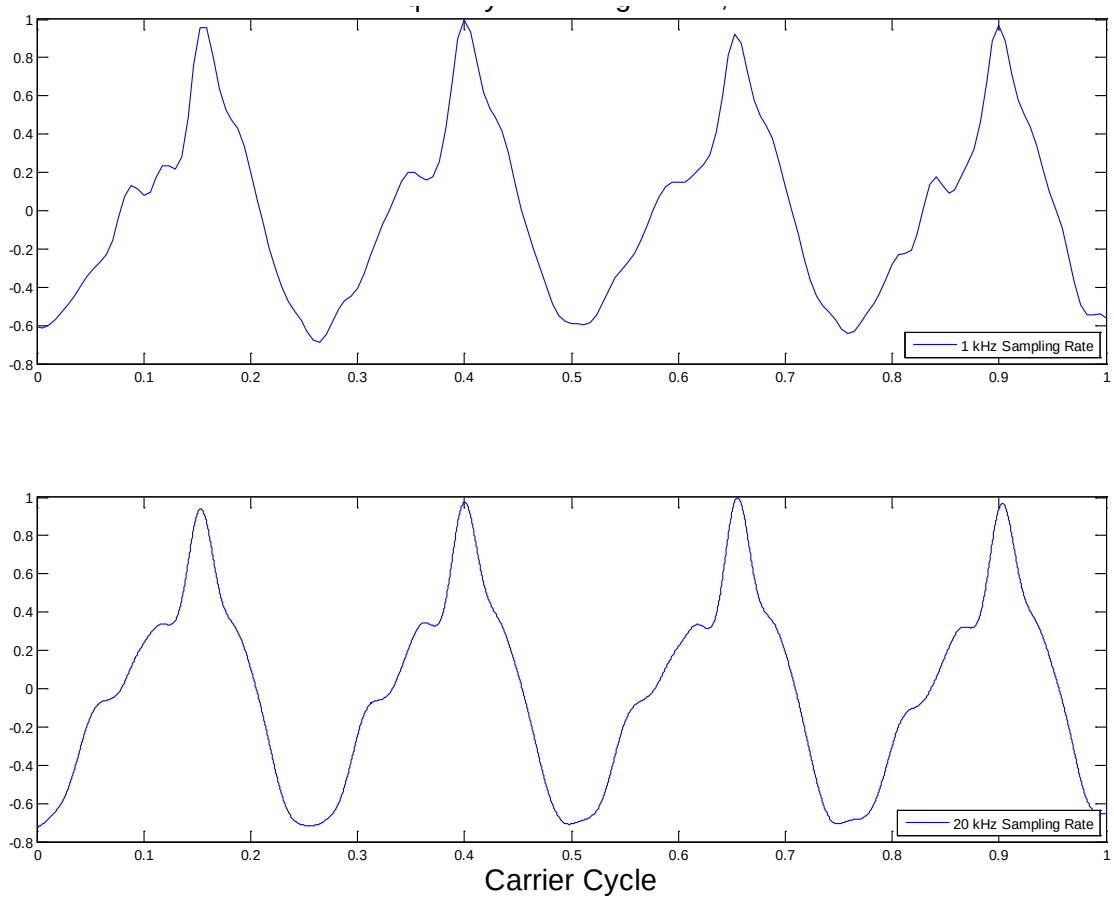

Figure 5: Low frequency component of data collected over 1 carrier rotation: 1 kHz sampling rate (top) and 20 kHz sampling rate (bottom)

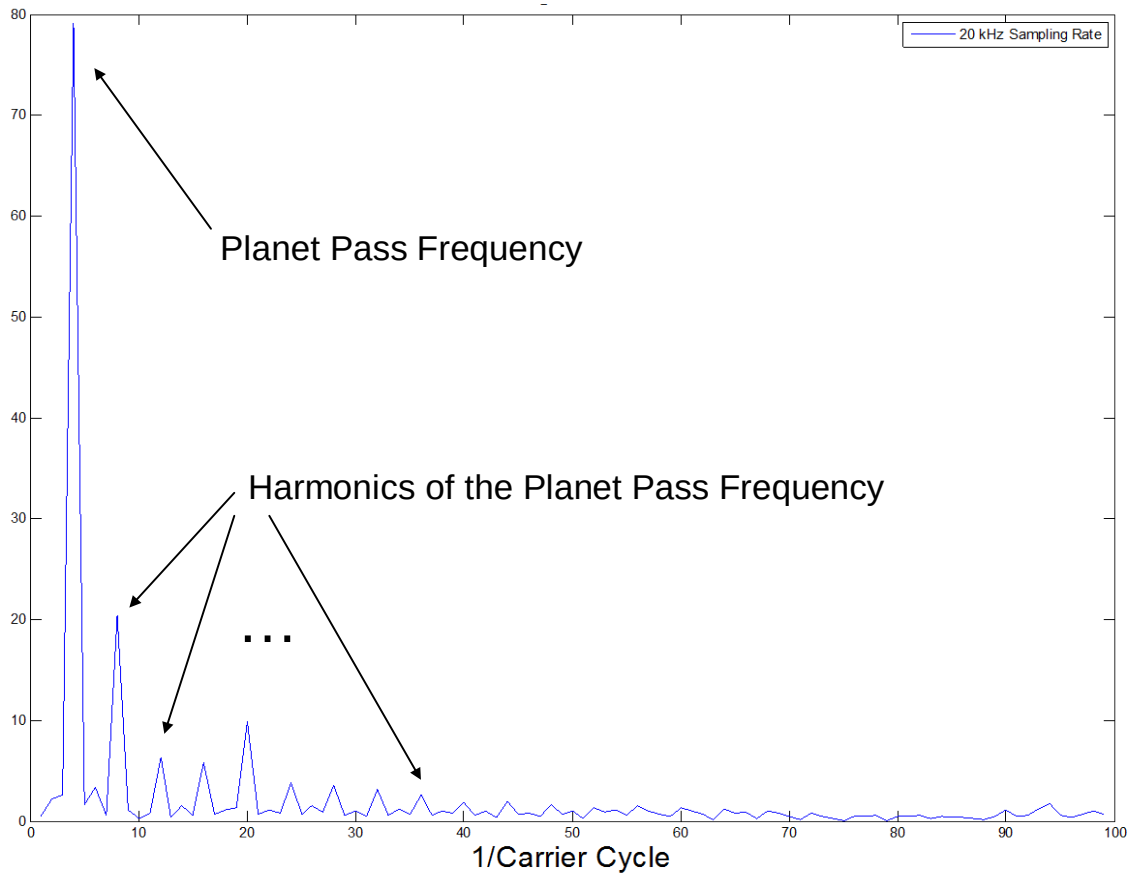

Figure 6: Spectrum of raw data collected sampled at 20 kHz. Low frequency range highlighted to show planet pass frequency.

The spectrum of the high sampling rate signal is shown in Figure 6 and Figure 7. Figure 6 presents the low frequency range of the raw data, and clearly shows that the planet pass frequency and harmonics are still easily captured. Figure 7 presents the spectrum of the high frequency component of the signal, and once again shows that good separation is achieved between the low and high frequency signals. In addition, it is evident that multiple harmonics of the mesh frequency are clearly captured. Finally, Figure 8 presents a comparison of the spectra of the high frequency components of the 1 kHz and 20 kHz data. This figure clearly indicates that an increase in the sampling rate enables the fiber optic strain sensors to clearly capture high frequency features of the vibration signal, and would make damage detection at the normal operating RPM possible since the mesh frequency is now captured.

Overall, these initial characterization results indicate that an increase in sampling rate would enable damage detection to be performed at the normal operating RPM of the OH-58C transmission. In addition, it suggests that the strain sensors are able to capture high frequency features of the signal, and thus damage detection results could be improved. It is recommended that the use of high sampling rate strain data for helicopter transmission damage detection be investigated in a future research program.

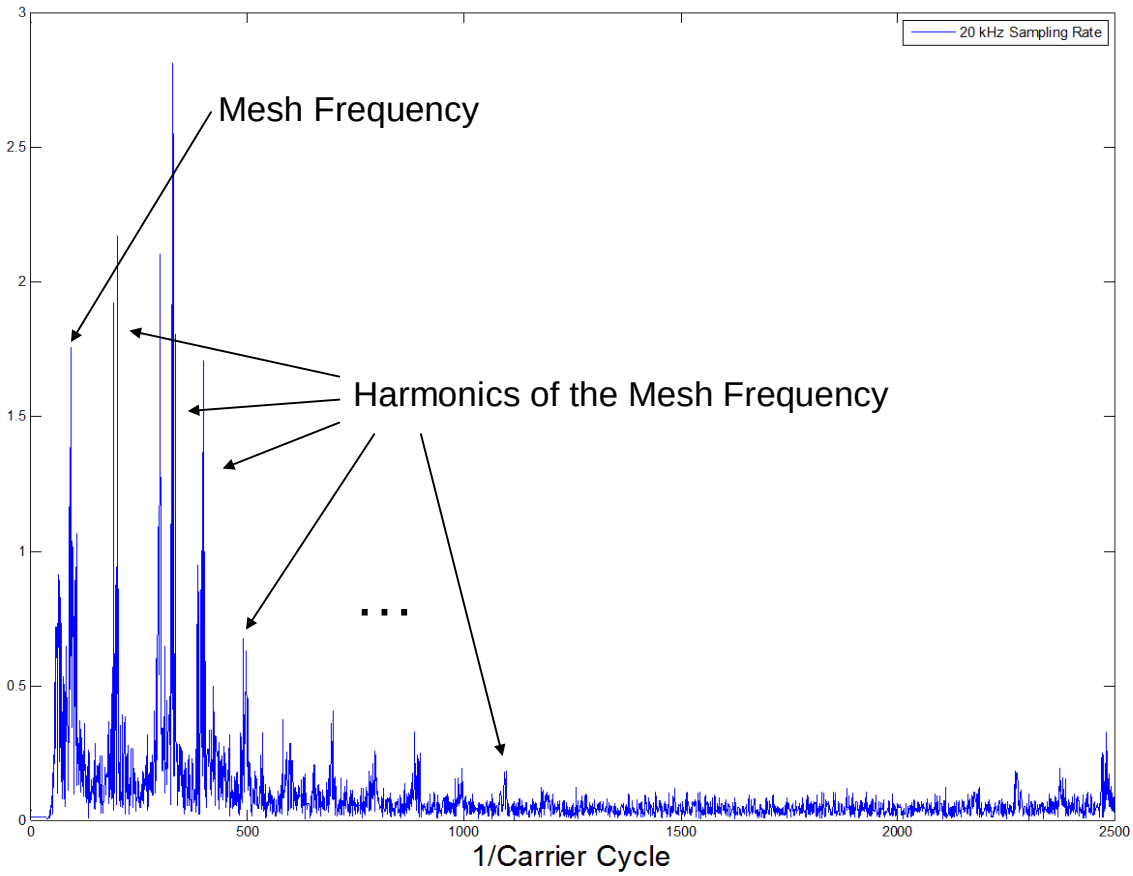

Figure 7: Spectrum of high frequency component of data sampled at 20 kHz.

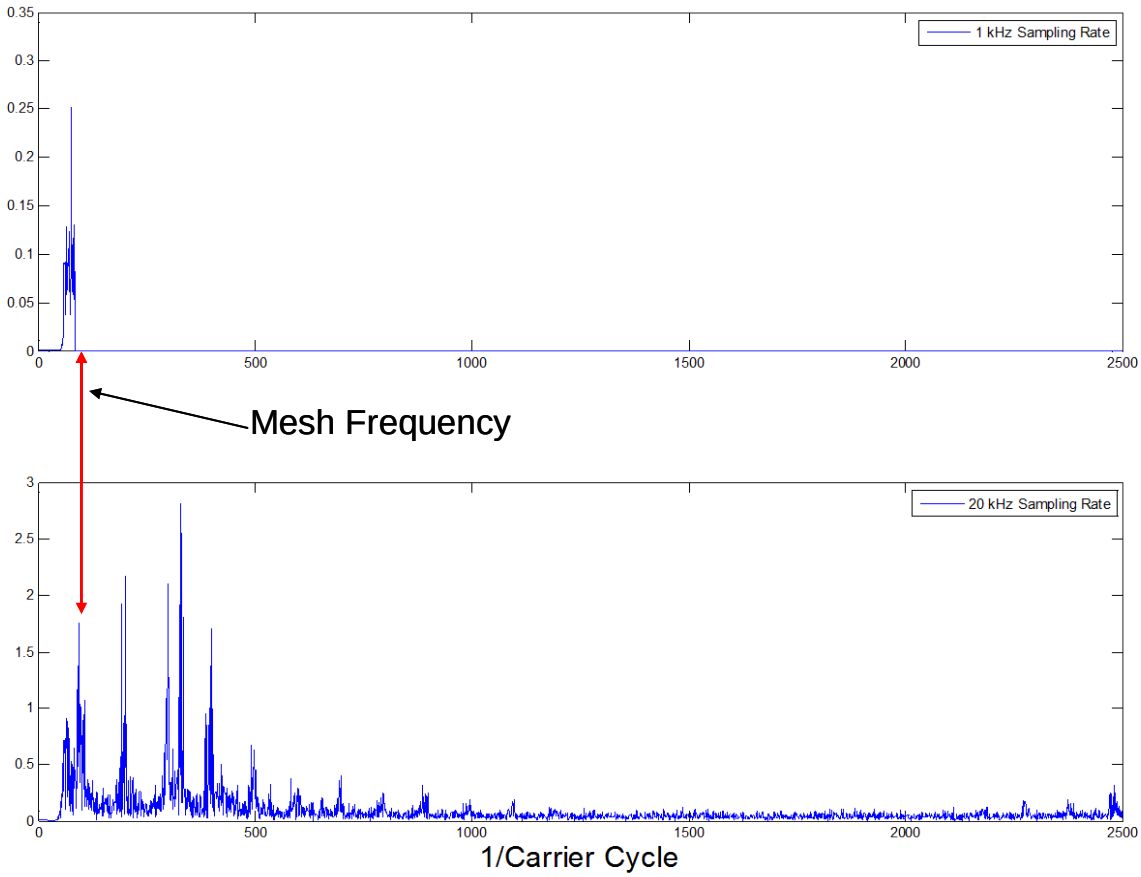

Figure 8: Comparison of spectra of high frequency component of data sampled at 1 kHz (top) and 20 kHz (bottom)

4. COMMERCIALLY AVAILABLE INSTRUMENTATION

The discussion above illustrates the goals of the monitoring system to maximize the sampling rate along with the number of serially multiplexed sensors. However, these two goals often compete, making it difficult to reach the desired sampling rates with a good number of multiplexed sensors. Throughout this research effort, Aither has investigated interrogation systems with higher sampling rates. This section provides an overview of some commercially available high sampling rates to illustrate the current state of art.

The fiber optic interrogation system used throughout the current effort was the Micron Optics' sm130, which has a maximum sampling rate 1 kHz (2 kHz with a reduced wavelength range). This unit allows for sampling of serially multiplexed FBG sensors over an 80 nm optical bandwidth. For the current sensor design, only 13 FBG sensors were integrated along 50 nm of the optical bandwidth, therefore additional sensors could be added to fill out the 80 nm bandwidth. The FBG sensors could also be placed with a high wavelength density, since testing as shown that there is minimal thermal variation along the sensor array (all FBG sensors similarly to temperature variations). Based on the observed behavior of the FBG sensors, a total of 20 serially multiplexed sensors could be placed on the band within the 80 nm optical bandwidth being sampled at 1 kHz. Micron Optics has released an alternative version of the sm130 that allows for 2 kHz sampling rate but only has a 40 nm optical bandwidth; thus reducing the total number of serially multiplexed sensors.

Micron Optics' si920

The Micron Optics' si920 has the highest sampling rate of any of the interrogators at 500 kHz [8]. However, this high sampling rate is only available for a single FBG sensor per fiber. The unit has four optical channels and can interrogate all four simultaneously (four total FBG sensors) at a rate of 100 kHz. This unit would provide a more than adequate sampling rate for the monitoring system, but the requirement for each FBG sensor to be dedicated to a single optical fiber would lead to a very difficult egress from the transmission housing.

Figure 9: Micron Optics' si920 Instrumentation System [8]

Smart Fibres SmartScan

The Smart Fibres SmartScan Dynamic FBG Interrogator allows for a user defined sampling rate that is dependent on the optical bandwidth selected by the user. The default setting on the SmartScan instrument is to have an optical bandwidth of 40 nm (maximum for the unit) resulting in a sampling rate of 2.5 kHz [9]. With a 40 nm optical bandwidth, a total of ten FBG sensors could be serially multiplexed for the ring gear application. The interesting attribute of the SmartScan system is the ability to change the optical bandwidth and increase the sampling rate of the system. Changing the optical bandwidth is performed on all four optical channels of the SmartScan system, so all FBG sensors must fall within the user selected bandwidth. During testing with the current research effort, a 20 kHz sampling rate was used. However, the optical bandwidth was reduced to the point where only two FBG sensors could be interrogated.

Figure 10: Smart Fibres' SmartScan Interrogator [9]

Technobis Fibre Technologies' Deminsys FBG Interrogator

Technobis Fibre Technologies Deminsys FBG interrogator utilizes a CCD imager to capture the reflected FBG signals [10]. The imager is sensitive to light at a different wavelength then the other interrogators discussed. The wavelength range for this unit is 830 to 870 nm (40 nm optical bandwidth). The other interrogators operate in the 1550 nm range. The system currently relies on the FBG sensors having certain wavelength values so the interrogator software knows where to bin the corresponding pixels on the imager. The interrogator is currently limited to 8 serially multiplexed FBG sensors per channel with a sampling rate of 20 kHz.

Figure 11: Technobis Fibre Technologies' Deminsys FBG Interrogator [10]

Light Structures FRIMP

Light Structures has an FBG interrogation system that consists of 8 optical fiber channels where each channel interrogates a single FBG sensor [11]. The demodulation system is based on an interferometric technique and allows for a sampling rate of 20 kHz for each FBG sensor.

5. SUMMARY

This paper presented results from FBG sensors mounted to a ring gear in the NASA Glenn Research Center OH-58 transmission test rig facility. The overall purpose of this research effort was to evaluate the ability of the recorded FBG response data to detect damage for various cases using damage detection algorithms. During the testing effort, it became clear that higher sampling rates would be beneficial for the damage detection system. The fiber optic sensor setup used in the research effort included a serially multiplexed sensor array of 13 FBG sensors. A Micron Optics' sm130 interrogator with an acquisition rate of 1 kHz was used throughout the effort. Data was also collected using a Smart Fibres' Smart Scan system at 20 kHz, with only two of the FBG sensors being recorded due to the reduced optical bandwidth. In general, a trade-off exists between sampling rate and the number of serially multiplexed FBG sensors. Based on testing during this effort and other damage detection techniques, the recommended sampling rate for the transmission damage detection system is 50 kHz. The number of FBG sensors to be sampled simultaneously at this rate is on the order of 20. Further testing with higher sampling rate systems is recommended to further evaluate the system requirements.

REFERENCES

1. P. D. McFadden, "A technique for calculating the time domain averages of the vibration of the individual planet gears and sun gear in an epicyclic gearbox," Journal of Sound and Vibration, 144(1), pp.163–172, 1991.
2. D. Forrester, "A method for the separation of epicyclic planet gear vibration signatures" in Proceedings of Acoustical and Vibratory Surveillance Methods and Diagnostic Techniques, pp. 539–548, Senlis, France, October 1998.
3. P. D. Samuel and D. J. Pines, "Vibration separation and diagnostics of planetary geartrains," in Proceedings of The American Helicopter Society 56th Annual Forum, Virginia Beach, Va, May 2000.
4. C. S. Baldwin, et al. "Fiber Optic Sensors Monitoring Transmission Ring Gears," Proceedings SPIE Optics East Conference, Boston, MA, 2007.
5. J. S. Kiddy, et. al., "Fiber Optic Strain Sensor for Planetary Gear Diagnostics," American Helicopter Society 67th Annual Forum, Virginia Beach, VA, 2011.
6. Othonos, A. and Kalli, K., Fiber Bragg Gratings: Fundamentals and Applications in Telecommunications and Sensing, Artech House, Inc., 1999.
7. J. K. Conroy, P.D. Samuel and D.J. Pines. Development of a real-time LabVIEW-based testbed for implementation of planetary gear diagnostic algorithms. In Proceedings of the AHS 59th Annual Forum, Phoenix, Az, May 2003.
8. http://www.micronoptics.com/uploads/library/documents/Datasheets/si920%20-Micron%20Optics-%200809.1.pdf
9. http://www.smartfibres.com/docs/SmartScan.pdf
10. http://www.technobis-fibre-technologies.nl/files/145_Deminsys.pdf
11. http://www.lightstructures.biz/images/stories/pdf/frimptech_20khz.pdf

ACKNOWLEDGEMENTS

This research was partially funded by the Government under Agreement No. W911W6-07-2-0003. The U.S. Government is authorized to reproduce and distribute reprints for Government purposes notwithstanding any copyright notation thereon. The views and conclusions contained in this document are those of the authors and should not be interpreted as representing the official policies, either expressed or implied, of the Aviation Applied Technology Directorate or the U.S. Government.

Aither Engineering would also like to thank Smart Fibres for providing a demonstration system of the Smart Scan interrogator for this research effort.